LA-UR- 96-3118

TITLE: **SURFACE MODIFICATION OF AISI-4620 STEEL WITH INTENSE PULSED ION BEAMS**

AUTHORS: D.J. REJ, H.A. DAVIS, M. NASTASI, J.C. OLSON, E.J. PETERSON, R.D. REISWIG, K.C. WALTER R.W. STINNETT, G.E. REMNEV, V.K. STRUTS

SUBMITTED TO: *10th Intern. Conf. on Ion Beam Modification of Materials Albuquerque, NM Sept. 1-6, 1996*

*Nuclear Instruments and Methods in Physics Research B*



**Los Alamos**
NATIONAL LABORATORY



Form No. 836 R5
ST 2629 10/91

## DISCLAIMER

## DISCLAIMER

Portions of this document may be illegible in electronic image products. Images are produced from the best available original document.

# SURFACE MODIFICATION OF AISI-4620 STEEL WITH INTENSE PULSED ION BEAMS

D.J. Rej, H.A. Davis, M. Nastasi, J.C. Olson,[a]

E.J. Peterson, R.D. Reiswig, and K.C. Walter

*Los Alamos National Laboratory, Los Alamos, NM 87545 USA*

R.W. Stinnett

*QM Technologies, Inc., 3701 Hawkins NE, Albuquerque, NM 87109 USA*

G.E. Remnev and V.K. Struts

*Nuclear Physics Inst., 2a Lenin Ave., Tomsk 634050, Russia*

## ABSTRACT

A 300-keV, 30-kA, 1-μs intense beam of carbon, oxygen, and hydrogen ions is used for the surface treatment of AISI-4620 steel coupons, a common material used in automotive gear applications. The beam is extracted from a magnetically-insulated vacuum diode and deposited into the top 1 μm of the target surface. The beam-solid interaction causes a rapid melt and resolidification with heating and cooling rates of up to $10^{10}$ K/sec. Treated surfaces are smoothed over 1-μm scale-lengths, but are accompanied by 1-μm diameter craters and larger-scale roughening over ≥10 μm, depending on beam fluence and number of pulses. Treated surfaces are up to 1.8× harder with no discernible change in modulus over depths of 1 μm or more. Qualitative improvements in the wear morphology of treated surfaces are reported.

## I. INTRODUCTION

High-intensity pulsed ion beam technology has been developed over the last two decades primarily for nuclear fusion and high-energy density physics research [1]. An intense ion beam is usually created in a magnetically-insulated vacuum diode [2] from which a 10 to 1000 kA beam of low-Z ions are accelerated to energies typically between 10 keV and 10 MeV over a 10 to 1000 ns pulse. The beam may be extracted, focused, and propagated to interact with a solid material. This emerging technology has also proven to be a unique pulsed energy source for the surface modification of materials [3]. For example, direct deposition of a beam into the top 1 to 10 μm of a solid surface results in a rapid melt and resolidification with heating and cooling rates of up to $10^{10}$ K/sec. These rates are sufficiently high to promote mixing, rapid diffusion, and the formation of amorphous surface layers. The intense beam process is similar to surface modification with high-power lasers and electron beams. Advantages of intense ion beams include their high overall efficiency (15-40% of wall plug energy can be converted to beam), better coupling to target materials, and larger cross sectional area (typically 50 to 1000 $cm^2$). Unlike laser processing, however, a medium-grade vacuum ($10^{-4}$ Torr or lower) is required and x-ray shielding must be provided.

In this paper we report preliminary results from ion beam surface treatment (IBEST) experiments aimed at improving the surface mechanical properties of AISI-4620 steel. This material has been chosen because of its relatively simple composition, its widespread use in gear applications, and because it is commonly treated with conventional surface modification methods such as heat treatment or carburizing.

## II. EXPERIMENTAL

The target material consisted of AISI-4620 steel coupons (composition > 96% wt. Fe, 0.2% C, 0.55% Mn, 1.8% Ni, 0.25% Mo, 0.3% Si, ≤ 0.04% S, ≤ 0.04% P). Coupons were mechanically polished to $R_a \approx 0.1$ μm. Experiments were performed on the Los Alamos Anaconda accelerator [2]. A 300-keV, 30 kA, 1-μs pulsewidth beam of C, O, and H ions was generated, propagated 0.4 m, and injected into the coupons. Samples were irradiated with either N = 1, 3, or 10 pulses at incident energy fluences q of either 2 or 5 J/cm$^2$ per pulse.

Beam-solid interactions were modeled by numerical solutions to the one-dimensional heat equation. Target heating was estimated by distributing the incident beam power density into the surface with a deposition profile determined from *TRIM* code simulations [4]. Phase transitions, temperature-dependent heat capacities and thermal conductivity were included. As illustrated in Fig. 1, the model predicted target melting at both q values, while surface evaporation was expected only at 5 J/cm$^2$.

Composition and microstructure of the coupons were evaluated with scanning electron microscopy (SEM) and x-ray diffraction (XRD). Melt and heat-effected zones were examined with conventional metallographic techniques, while surface texturing was studied with profilometry using a 25-μm-diam stylus and optical microscopy. Surface hardness was measured with Knoop indentation with a 100-g load, and with nanoindentation performed in the continuous stiffness mode. Accelerated pin-on-disk wear tests were completed with a 6-mm-diam ruby ball at 0.8 N load 200 rpm, 50% rh, 3-mm track diameter, and 3-mm/s sliding speed over 60-minute intervals.

## III. RESULTS

Surface modification is observed at all conditions. At N=10 and q = 5 J/cm$^2$, a non-uniform surface layer between 0.2 and 1 μm thick (Fig. 2) is interpreted to be the melt zone. This region is backed by a non-uniform heat-effected zone between 1 and 5-μm thick. SEM and optical microscopy show smoothing over micron scale-lengths, as evidenced by the removal of the polishing marks in Fig. 3. Microsmoothing is accompanied by large-scale (≥ 10-μm) roughening, dependent on treatment conditions. At N=1 and q=5 J/cm$^2$, profilometer scans reveal an increase in surface roughness ±1 μm over a ≤ 100 μm scale-length. Optical microscopy reveals a cellular structure over this scale. For N=10, roughness increases to ±2 μm, but over a coarser, 200-300 μm scale-length. Qualitatively similar trends are observed at 2 J/cm$^2$.

The IBEST process generates 1-μm-diam craters in the target surface (Fig. 4). The highest number of craters is observed after 1 or 3 pulses at both fluences. The number of craters is noticeably smaller after 10 pulses at 5 J/cm$^2$.

XRD profiles are shown in Fig. 5. The increased background at low θ is due to scatter from an epoxy mounting material. The virgin sample displays a body-centered crystalline structure consistent with BCC ferrite (α-Fe) or BCT (α'-Fe) martensite, with a=2.871(1)Å. These data are interpreted to be indications of martensite since the characteristic $Fe_3C$ orthorhombic (cementite) peaks, which often accompany α-Fe, are not observed. This interpretation is consistent with the surface hardness discussed below. The sample treated at N=10, q=5 J/cm$^2$ is composed of a mixture of α'-Fe (a=2.869(1)Å) and austenite (γ-Fe,

FCC, a=3.612(4)Å), with the diffraction pattern showing three fairly broad austenite peaks. The expected intense (111) austenite peak that should be located at $2\theta \approx 43.4°$ is not seen.

Knoop indents exhibit a 1.4× increase in surface hardness from 337±27 kg/mm$^2$ for the untreated sample to 466±30 kg/mm$^2$ at N=10 and q= 5 J/cm$^2$ (corresponding to average indent depths of 2.2 and 1.8 μm, respectively). Nanoindentation hardness in the outermost μm surface shows a softening for N=1 and q= 5 J/cm$^2$, and hardening up to 1.8× at N= 3 and 10 pulses, with no discernible change in elastic modulus (Fig. 6).

Treated surfaces have a substantially different wear morphology. Fig. 7 shows SEM images of wear tracks following the pin-on-disk tests. The data show a reduction in the amount of surface plastic deformation indicating a reduction in the adhesive and abrasive wear. The relatively high surface roughness caused by the treatment prevented accurate profilometer measurements of the wear coefficient, while friction coefficients varied between 0.5 and 0.8.

## IV. DISCUSSION

These preliminary experiments indicate that rapid melt and resolidification with intense pulsed ion beams can smooth steel surfaces on a microscopic scale. The melt zone thickness is consistent with the calculations, although large variations in depth are observed. Both surface hardening and softening are seen depending on treatment conditions. These observations are not fully understand at this time, although one can speculate that competing processes are at work, *e.g.*, softening due to the formation of retained austenite (observed in the XRD), and hardening due to grain refinement and dislocation formation (common in IBEST processing [5]).

Surface damage from craters formed during IBEST could pose limitations in applications. It is conjectured that craters may result from selective heating of impurity material, resulting in

ablation at the target surface or subsurface bubble formation which subsequently leads to surface fracture. Recent studies [6] with high-power electron beams support this speculation in that the craters are agglomerated in chains, possibly due to the ablation of impurities that often concentrate near grain boundaries. Furthermore, craters tend to disappear after multiple electron beam pulses, being completely eliminated after approximately 100 pulses. Similar trends are evident in these experiments when one compares the N=3 and 10; however, further work is needed to better characterize crater formation.

The observation of some retained austenite in the treated sample is consistent with the conversion of some martensite to austenite during the surface heating followed by rapid cooling to quench the austenite phase. The martensite lattice parameter is unchanged (within error) by the treatment. The absence of the austenite (111) peak in the treated sample may be the result of a preferred orientation of the austenite. Alternatively, because the (111) plane contains the highest atom density, selective amorphization of crystals with [111] orientations may have occurred. Broadening of the diffraction peaks (both martensite and austenite) in the treated sample is consistent with damage to the crystal structure by amorphization or induced strains. The anomalously large fwhm of the (310) peak in the treated sample may be due to overlap with the austenite (400) peak.

The wear morphology of the treated steel is qualitatively different. Severe wear is evident on the untreated material, consistent with a true Hertzian contact stress which exceeds the flow stress of the material. The nature of the plastic deformation present in the wear scares suggests that plowing may be the predominant abrasive wear mechanism operating which is supported by the high friction coefficients observed.

These observations are consistent with IBEST processing of α-Fe and type 35 steel (≥ 98% Fe, ≤ 0.35% C, 0.65% Mn, ≤ 0.25% Ni, ≤ 0.27% Si, ≤ 0.25% Cr) performed with $q \leq 2.1$ J/cm$^2$ on the TEMP accelerators in Tomsk. TEMP [7] generates beams with similar parameters as Anaconda but with shorter, 50-ns pulsewidths; consequently, surface melting is obtained at lower q, since there is less diffusion into the target from thermal conduction. Microsmoothing and large-scale roughening (0.5 to 1.5 μm) of surfaces are observed with both materials. Microsmoothing without crater formation is observed at low fluences $q \approx 0.9$ J/cm$^2$, with craters detected only at higher fluences $q \geq 1.5$ J/cm$^2$ on TEMP.

## ACKNOWLEDGMENTS

This research is sponsored by the U.S. Dept. of Energy Defense Programs through their Technology Transfer Initiative Small Business Staff Exchange Program, and through their U.S.-Former Soviet Union Industrial Partnership Program.

[a] Present address: Varian Ion Implant Systems, 508 Dory Rd., Gloucester MA 01930

## REFERENCES

[1] J.P. VanDevender and D.L. Cook, *Science* **232** (1986) 831.

[2] D.J. Rej *et al.*, *Rev. Sci. Instr.* **64** (1993) 2753.

[3] H.A. Davis, G.E. Remnev, R.W. Stinnett, and K. Yatsui, *MRS Bulletin* **21** (1996) 58.

[4] J. F. Ziegler, J. P. Biersack, and U. Littmark, *The Stopping and Range of Ions in Solids* (Pergamon Press, New York, 1985).

[5] A.D. Progrebnjak and Sh.M. Ruzimov, *Phys. Lett.* **A120** (1987) 259.

[6] D.I. Proskurovsky, V.P. Rotshtein, G.E. Ozur, submitted to *Surf. Coat. Technol.*

[7] I.F. Isakov *et al.*, *Vacuum* **42** (1991) 159.

## FIGURE CAPTIONS

1. Predicted time evolution of temperature T(x,t) in the near surface of 0.5% carbon steel after being irradiated with the Los Alamos intense ion beam with fluences of (a) 2 and (b) 5 J/cm$^2$. The initial, melting, vaporization, and ablation temperatures are 300, 1800, 3270, and 3628 K, respectively.

2. Cross-sectional SEM image of an AISI-4620 steel coupon after 10 ion beam pulses at 5 J/cm$^2$. The treated coupon was sectioned with a low-speed diamond wafer blade, mounted in epoxy, ground and polished with diamond and alumina abrasives (from 30 to 0.3 μm), and etched in 1% Nital.

3. Secondary emission SEM image of (a) untreated and (b) treated (10 pulses at 5 J/cm$^2$) coupon.

4. Secondary emission SEM image of a crater in surface treated with 10 pulses at 5 J/cm$^2$.

5. XRD profiles of untreated and treated (N = 10, q = 5 J/cm$^2$) coupons.

6. Nanoindentation profiles of (a) hardness and (b) modulus for IBEST treated coupons at 5J/cm$^2$.

7. SEM images of the wear tracks after identical pin-on-disk tests on (a) untreated and (b) treated (10 pulses at 5 J/cm$^2$) surfaces.

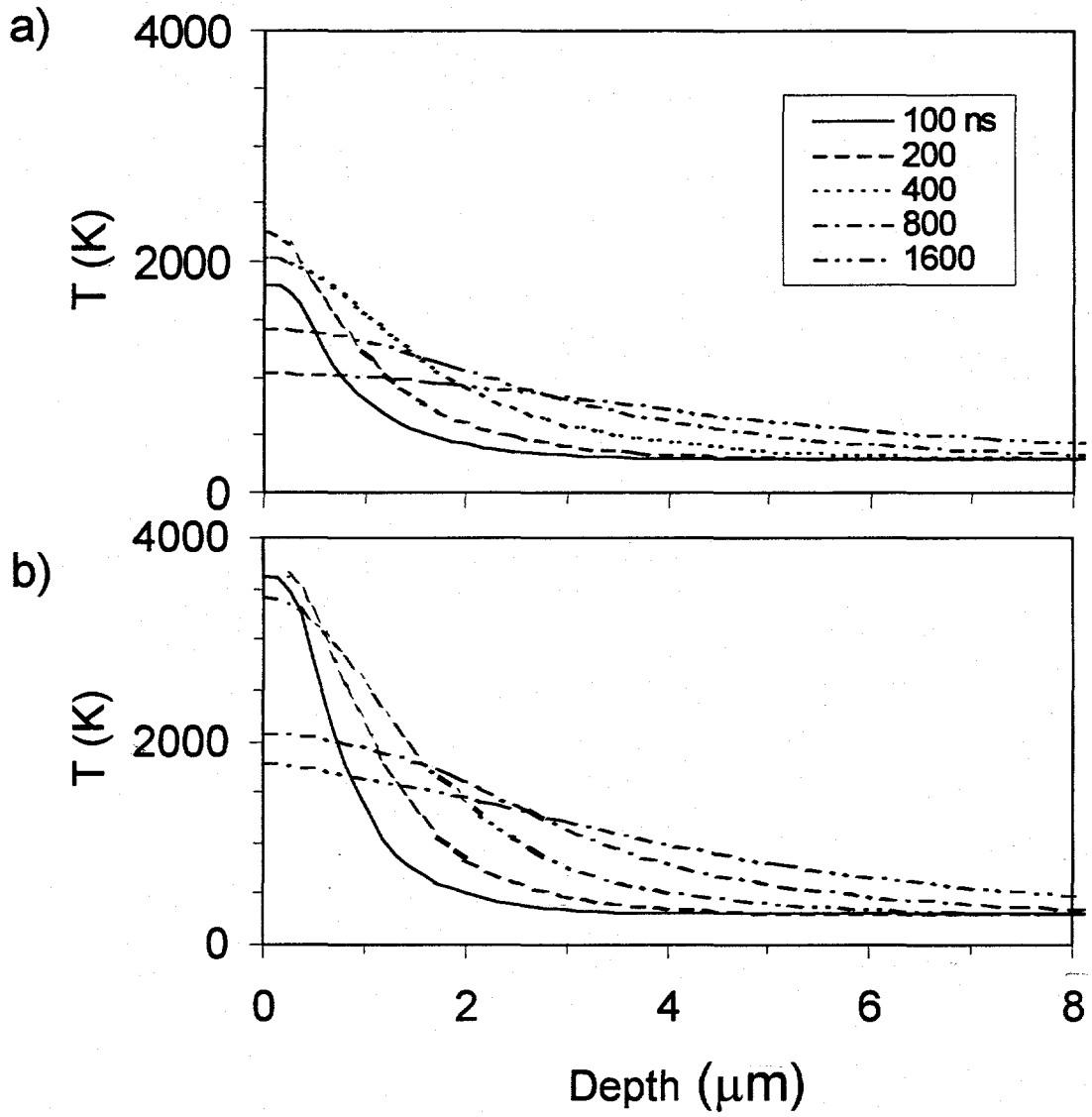


D. J. Rej *et al.*, Fig. 1

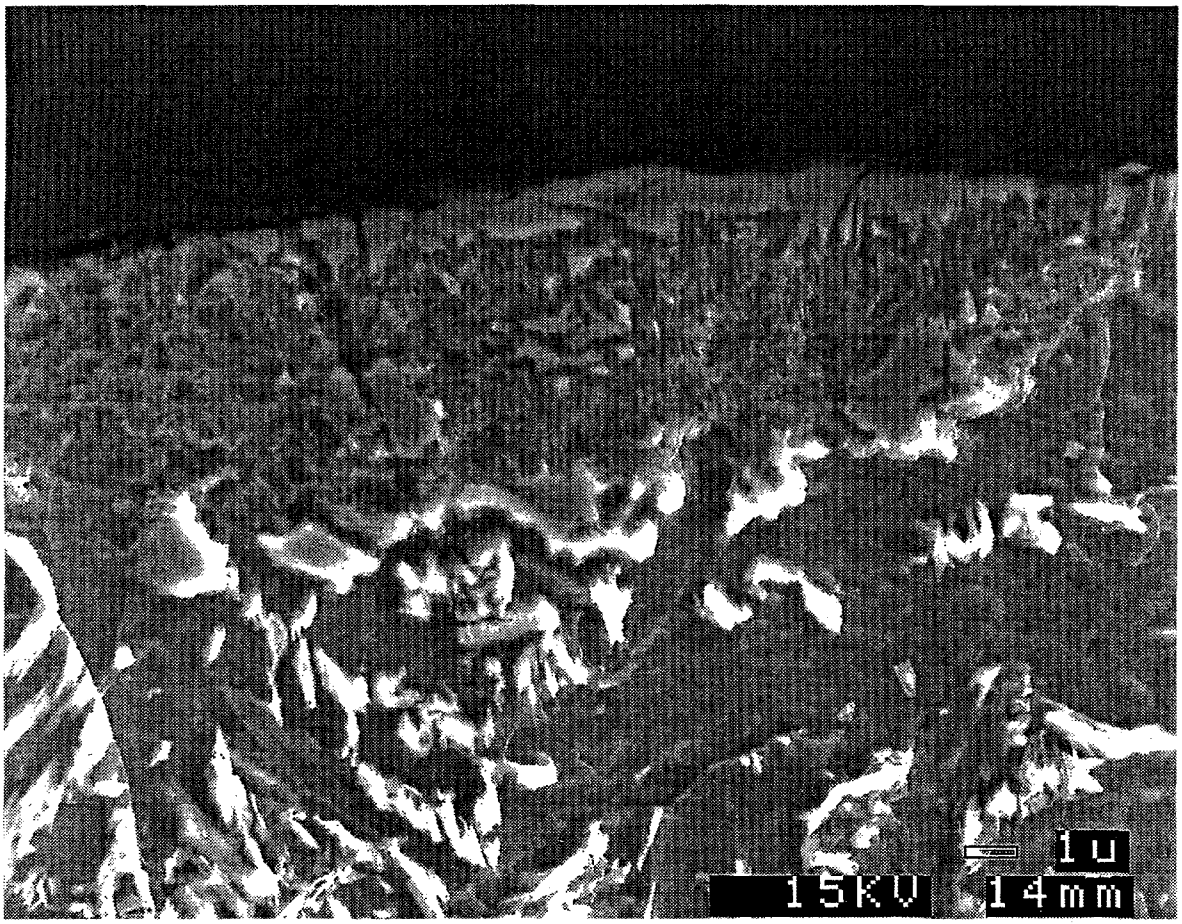


D. Rej *et.al.* Figure 2

a)

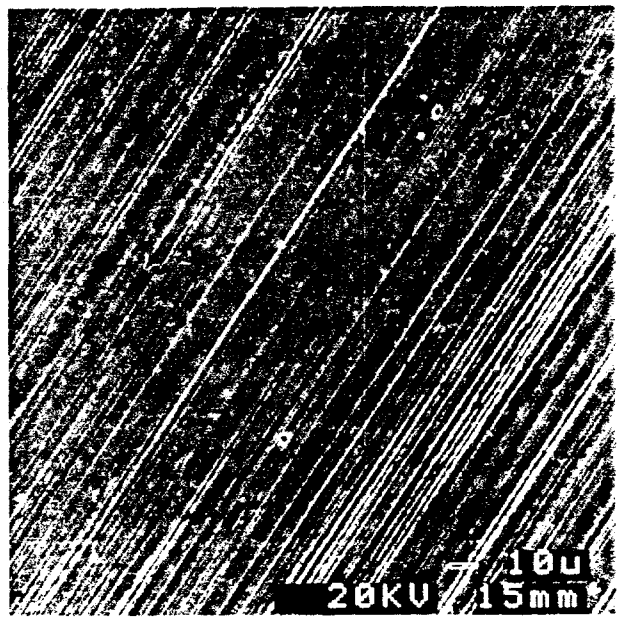


b)


D. Rej *et.al.* Figure 3


D. Rej *et.al.* Figure 4

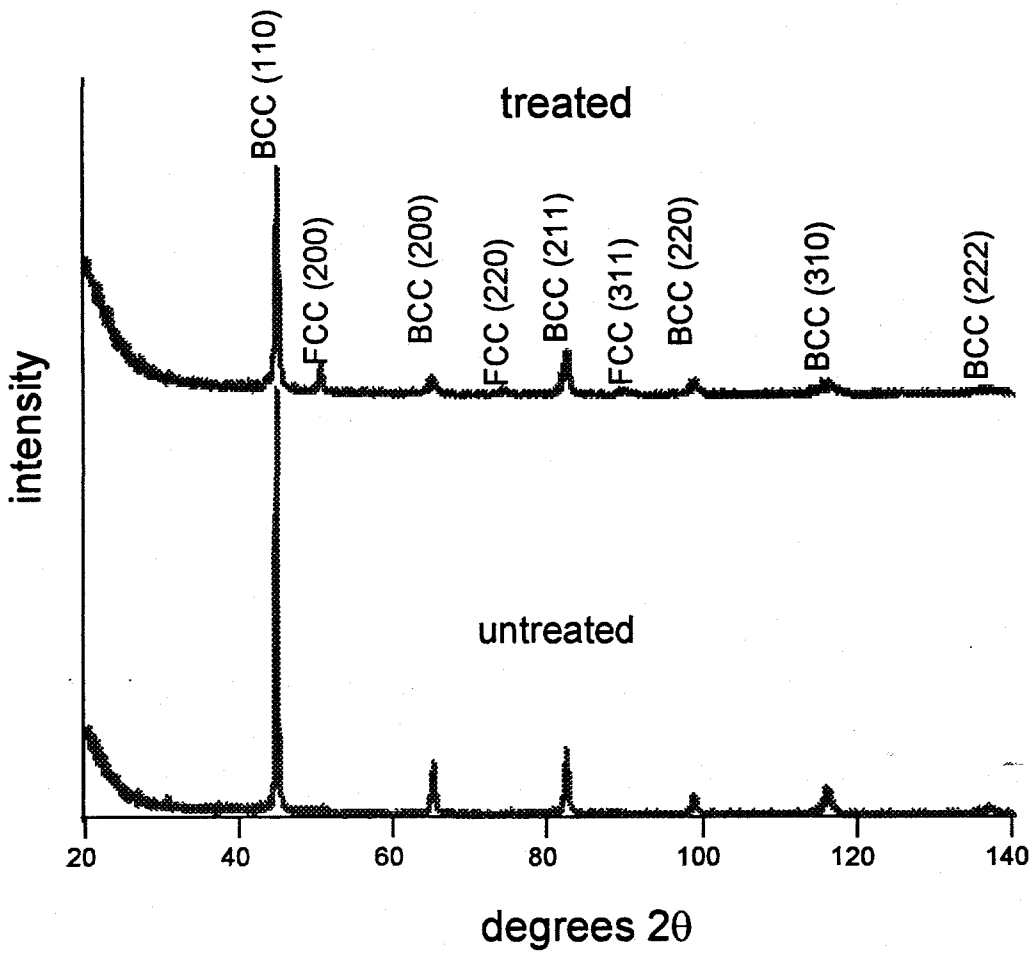


D.J. Rej *et al.*, Fig. 5

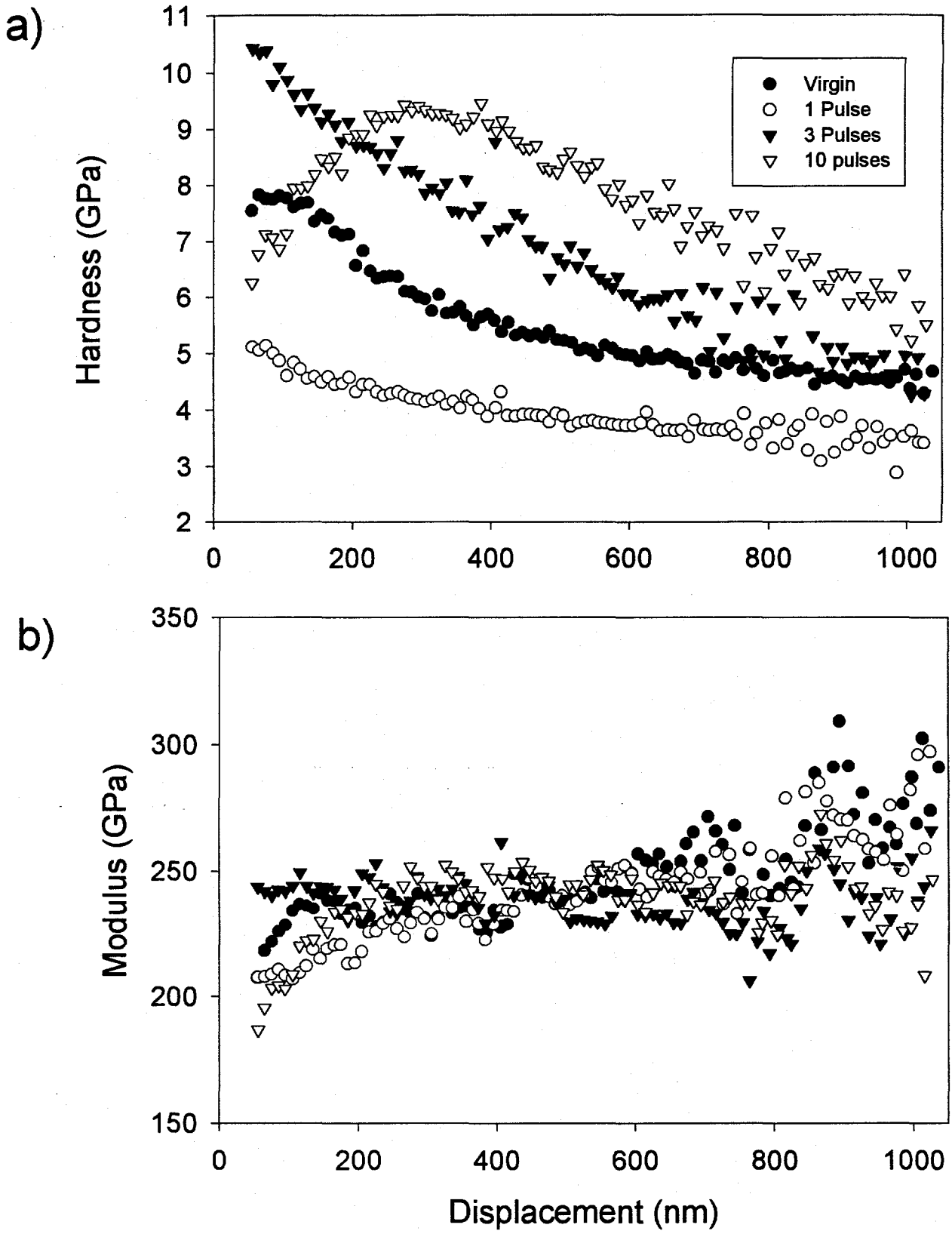


D.J. Rej *et al.*, Fig. 6

a)

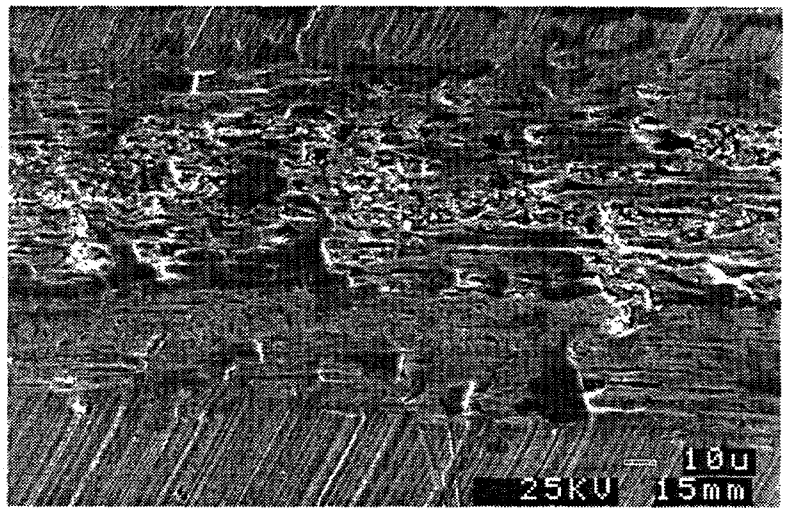


b)

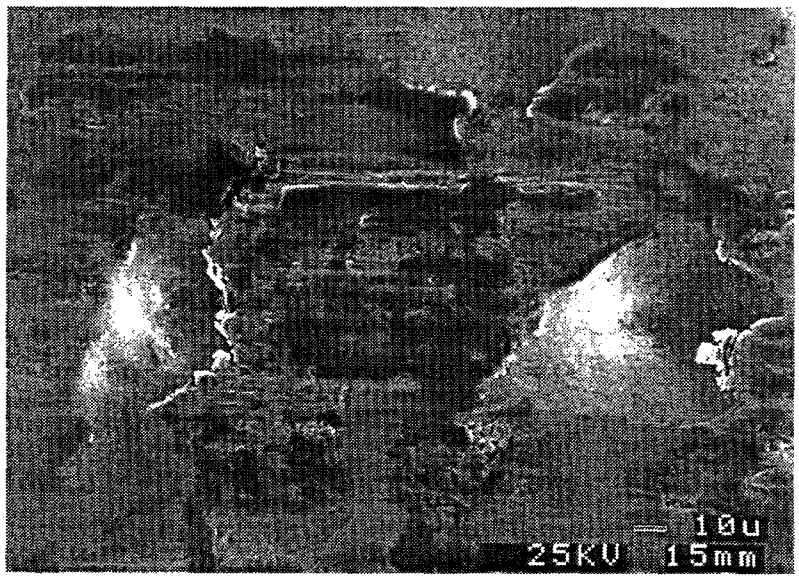


D. Rej *et.al.* Figure 7